

EUROPEAN ORGANIZATION FOR NUCLEAR RESEARCH

In-trap conversion electron spectroscopy.

CERN-EP/2002-011

7 February 2002

L. Weissman¹⁾⁵⁾, F. Ames¹⁾²⁾, J. Aysto¹⁾³⁾, O. Forstner¹⁾, K. Reisinger¹⁾²⁾, S. Rinta-Antila⁴⁾, and the ISOLDE and the REX-ISOLDE collaborations¹⁾

Abstract

The Penning trap REXTRAP at ISOLDE was used to test the feasibility of in-trap conversion electron spectroscopy. The results of simulations, experiments with solid conversion electron sources as well as first on-line and tests with trapped radioactive ions are presented. In addition to obtaining high-resolution spectroscopic data, the detection of conversion electrons was found to be a useful tool for the diagnostics of the trap operation. The tests proved the feasibility of in-trap spectroscopy but also revealed some potential problems to be addressed in the future.

¹⁾ CERN, CH-1211 Geneva 23, Switzerland

²⁾ Sektion Physik, LMU Munchen, D-85748 Garching, Germany

³⁾ Helsinki Institute of Physics, FIN-00014, Helsinki, Finland

⁴⁾ Department of Physics, University of Jyväskylä, FIN-40100, Jyväskylä, Finland

⁵⁾ corresponding author: leonid.weissman@cern.ch

present address: NSCL, Michigan State University, East Lansing, MI 48824-132

1 Introduction

The thickness of radioactive sources has always been a limiting factor of high-resolution electron spectroscopy due to scattering in the source material. In a typical electron spectroscopy setup a strong magnetic field is applied for efficient transport of the emitted electrons towards a detector. In this case electrons undergoing multiple scattering and losing a significant fraction of their energy are also transported to the detector resulting in a distorted line shape, poor energy resolution and peak to background ratio [1, 2].

Trapped radioactive ions may provide new possibilities in the spectroscopy of low energy electrons like such as conversion electrons, since the trapped ions form an ideal source without energy loss and scattering. In this case an improved line shape and a better peak to background ratio are expected, thus allowing to obtain new nuclear spectroscopic information. The utilisation of in-trap electron sources free from energy losses and chemical effects will also allow to introduce more accurate electron calibration standards.

The scope of possible applications of in-trap spectroscopy can be expanded significantly if high energy resolution is achieved. For instance, accurate measurements of electron binding energies could be performed or the natural line-width of electron levels can be measured [3]. Since the electrons in many cases are emitted from recoiling nuclei after β or α decay careful analysis of the line shape may reveal new information on half-lives of nuclear states or on β -neutrino correlations. The comparison of the conversion electron spectra from the trapped radioactive atomic and molecular ions may reveal chemical influence on the electronic wave functions [4]. Atomic inner-shell vacancies created by internal conversion or electron capture cause a cascade of Auger, shake-up and shake-off electrons [5]. High-resolution in-trap detection of electrons may open new opportunities for deeper understanding of these processes.

As an example of such a set-up one can mention We report here on the first measurements of radioactive decay of ions stored in a Penning trap. The setup used in these studies was REXTRAP [6], which is the first element of the REX-ISOLDE post accelerator [7].

2 Experiment

2.1 REXTRAP and the idea of the test.

REXTRAP is a large Penning trap which performs bunching and cooling of radioactive ions for the following post-accelerating steps of REX-ISOLDE. The trap is situated on a high voltage (HV) platform to slow down 60 keV ions from the ISOLDE on-line separator [9]. A strong magnetic field, produced by a superconducting magnet, and an electric trapping potential, created by a set of cylindrical electrodes, serve for trapping of the decelerated ions. The ions are cooled by collisions with argon buffer gas atoms. A radio frequency near to the ion's cyclotron frequency is applied to damp instabilities associated with the magnetron motion and to centre the desired ion species [8]. The application of buffer gas with a typical pressure of 10^{-4} - 10^{-5} mbar in the trap centre requires isolation of the different parts by diaphragms to provide differential pumping. The typical distribution of buffer gas pressure and trapping electric potential are presented in Fig 1 together with the magnetic field profile. A detailed description of REXTRAP can be found in [6].

The strong magnetic field inside the trap (3 Tesla in the centre region) transports conversion electrons emitted by the trapped ions within a limited cylindrical volume. The major part of the emitted forward electrons will pass the ejection diaphragm. Only a small fraction of electrons emitted at large angles, almost perpendicular to the beam axis, will

be reflected from a magnetic mirror which is formed by a maximum of the magnetic field profile at a distance of approximately 20 cm from the centre (Fig 1). The simulation of electron trajectories in the trap shows that almost 90 % of low-energy (below 20 keV) electrons emitted from the trap centre in forward direction will pass the 5 mm ejection diaphragm. The corresponding fraction for more energetic electrons is almost constant up to high energy values (≈ 1 MeV) and equals to $\approx 70\%$.

For the measurement a detector can be placed into the trap behind the exit diaphragm (Fig. 1). The geometrical and physical conditions of REXTRAP determine the choice of the detector for the test. For example, the presence of buffer gas in the trap and the limited geometry do not allow the use of a high resolution cryogenic detector. The small diameter of the 5 mm diaphragm determines the size of the sensitive detection area and the 5 cm internal diameter of the trapping electrodes tube determines the overall size of the detector assembly. The high electron transport efficiency allows the efficient use of a detector with a small active area. The transport efficiency of electrons emitted from an ion cloud of 1 mm diameter to a 3 mm diameter detector placed behind the diaphragm is shown in Fig. 2. The simulations were done with the program SIMION [10]. A placement of the detector far from the source allows to reduce the background from X-rays and γ radiation coming from the ion cloud itself and from contaminations on the confining walls. Naturally, the best possible detector energy resolution is highly desired in order to investigate all possibilities of in-trap spectroscopy. A EB10GC-500P detector assembly together with a low noise PA1201 preamplifier of Canberra Semiconductor Ltd. has been used for the tests. The detector has a 10 mm² sensitive area (3.5 mm diameter) and 500 micron thickness. It is placed on a Peltier cooler together with a FET transistor, which serves as a first step of amplification. The detector dead layer is about 250 angstrom. Such detector assemblies are broadly used for X-ray spectroscopy and to our knowledge have not been used yet for electron measurements. The small size of the detector and close placement of the FET ensure low noise performance. A typical spectrum of a ²⁴¹Am source exhibits a resolution of less than 1 keV for the 59.5 keV X-ray line and a noise threshold of 3 keV (Fig 3a). These parameters can be only slightly improved by gentle cooling below 15-10 °C.

2.2 Measurements with electron sources.

Several tests with calibrated electron sources were performed. In first tests the detector assembly was placed in a test chamber without magnetic field together with calibrated ¹³³Ba, ¹³¹Ba and ²⁰⁷Bi electron sources. A typical electron spectrum of a ¹³¹Ba ($T_{1/2}=11.5$ days) source prepared by implantation of 60 keV ¹³¹Ba ions into a thin aluminium foil is shown in Fig. 3b. The spectrum exhibits resolution of 1.5-2 keV for the electron lines depending on the electron energy. The intrinsic efficiency of the detector measured with the calibrated sources is presented in Fig. 4 (full squares). Note that even at low energies the intrinsic efficiency is only 85 % due to backscattered electrons from the detector surface [11].

To perform tests with solid electron sources in the magnetic field the cylindrical electrodes and the diaphragms of the trap were taken out and a rigid detector-source assembly was introduced instead. The same distance between detector and source and the same position in the magnetic field as it was foreseen for the measurement of trapped ions was used. A PC based ADC was installed at the trap's HV platform and was used for data acquisition (DAQ). For the tests with solid sources no high voltage was applied to the platform. The measurements showed that the detector performance was not affected

by the strong magnetic field but the electron spectra exhibit a worse energy resolution (≈ 3 keV) and stronger low-energy background (Fig 3c). This is due to a larger spread in the electron energy losses in the source material as the electrons emitted at large angles with respect to the trap axis are also transported to the detector by the magnetic field. We have also observed a continuous β background from ^{207}Bi and ^{90}Sr sources, although the small detector thickness allows to detect the high energy β -particles only in “punch through” mode.

Measurements with the calibrated sources allowed to determine the absolute detection efficiency as a function of electron energy. The relative intensities of electron transitions from ^{207}Bi , ^{133}Ba and ^{131}Ba sources were taken from [12, 13]. The results are summarised in Fig 4, where the experimental efficiency (full circles) is compared with a calculated efficiency curve (solid line). To calculate the latter we have performed the convolution of the intrinsic detector efficiency measured in the test chamber (full squares and dashed line) with a calculated transport probability (Fig 2). The result of this convolution was corrected for a higher probability of electron backscattering from the detector’s surface and a higher probability of escape for electrons hitting close to the detector’s edge. Both effects are caused by a steep incident angle of electrons [11] moving at spiral trajectories in the magnetic field. The probability of detection of low-energy electrons backscattered from the detector and reflected from the magnetic mirror was also taken into account. As it is seen from Fig. 4, the calculation is in a reasonable agreement with the experimental results.

One has to point out the high detection efficiency even for our small area detector placed in the magnetic field. It can be compared to the absolute detection efficiency of a 200 mm^2 Si(Li) detector, for example the one used in the ELLI spectrometer [14]. At low electron energies the efficiency of the small detector in the magnetic field is much higher than that of the Si(Li) detector. For higher energies higher than 400 keV the efficiency of the small detector decreases due to the small detector’s thickness.

The obtained spectra are sensitive to the source position due to the small detector size. As the spiral radius of the electron’s trajectories is smaller for low-energy electrons the high-energy electron lines appear to be enhanced by a large factor when a source is shifted off-centre in the lateral direction. If nuclei with well known ratios for different electron lines are used this gives a possibility to perform diagnostics of the ion cloud. A shift of 5 cm of the whole detector-source assembly deeper inside the magnetic field increased the detection efficiency only by 15-20% whereas moving the assembly 5 cm out, i.e. outside the strong magnetic field reduces the efficiency by an order of magnitude.

2.3 On-line tests with fission product isomers.

To perform tests with trapped radioactive ions the cylindrical electrode structure and diaphragms were introduced back into the trap. The trap was optimised with beam of stable surface-ionised ^{138}Ba from a standard ISOLDE uranium-carbide (UC) target, heated to $2000\text{ }^\circ\text{C}$. A signal from a micro-channel plate (MCP) placed after the trap at ground potential was used to measure ions which were extracted from the trap after storage. After optimisation of the trap parameters with the MCP diagnostics the Si detector assembly was introduced. Thus, no independent further control of the trap performance was possible. The PC based data acquisition, placed on the high voltage platform, was connected to the external network via optical fibres. As soon as the high tension was applied we observed a background associated with stray electrons from the beam line. They are accelerated by the high tension applied to the trap platform (60 kV). The intensity of

the stray-electron background fluctuates strongly with time and depends on the pressure of the buffer gas and the intensity of the incoming beam. In case of a spark in the beam line the flux of accelerated stray electrons can be very intense and the summing peaks up to the seventh order together with a continuum background can be observed.

The choice of the radioactive ions for in-trap tests was limited to the well-known conversion electron emitters produced in proton-induced fission during bombardment of the UC target with 1 GeV protons from the CERN proton booster (PBS) facility. The production rate, a relatively short half-life and preferably a decay to stable daughter were the main factors limiting the choice of the nuclei used for the first test. The last two points are necessary to avoid an accumulation of longed-lived radioactivity in the trap. This would eventually result in an increasing background level. The fission products with isomeric transition (IT) isomer $^{116m2}\text{In}$ ($T_{1/2}=2.16$ s) and $^{118m2}\text{In}$ ($T_{1/2}=8.5$ s) were used for the first tests. The yields of surface ionised $^{116m2}\text{In}$ and $^{118m2}\text{In}$ were estimated to be 10^7 and $4\cdot 10^7$ ions per micro Coulomb of proton beam. The actual intensities of the ^{116}In and ^{118}In beams were approximately one order of magnitude higher due to the existence of β -decaying longer-lived isomers. During the test the trap cycle was set to 30 ms for collecting and accumulating of ions followed by 100 ms cooling, i.e. applying their cyclotron frequency. The trap cycle was synchronised with the PSB proton cycle that corresponded to 1 proton pulse in 16.8 second.

Several spectra were collected. A typical spectrum from the ^{116m}In isomer corresponding to the collections during 5 trapping cycles is shown in Fig 5a. One can observe a strong 60 keV and a much weaker 120 keV peak of accelerated stray electrons together with peaks at 20.1 keV 134.5 and 158.2 keV. The latter two correspond to the K- and unresolved M,L- lines of the 162 keV isomeric transition of $^{116m2}\text{In}$ whereas the 20.1 keV line corresponds to an Auger transition. The spectrum for $^{118m2}\text{In}$ taken with the same collection time and conditions is shown in Fig 5b where the 110 and 134 keV K- and unresolved L,M- electron lines can be observed. The ratio of intensities of the K-line and the sum of the unresolved L,M- lines is consistent with E3 multipolarity assignments for the IT transitions in both cases.

As it is seen from the spectra the obtained resolution is rather poor compared to the spectra from solid sources. It is about 4 keV and 6 keV for $^{116m2}\text{In}$ and $^{118m2}\text{In}$ respectively. One of the reasons is electronic noise caused by the utilisation of the ISOLDE laser ion source in an experiment, performed in parallel to the in-trap test. This however can not explain the worse resolution and higher background in the $^{118m2}\text{In}$ spectrum. A possible explanation is due to a factor 4 difference in the intensity of the two beams. The higher number of trapped ions may lead to a higher probability of summing of high-energy conversion electrons with low energy atomic electrons associated with the nuclear decay. Such a summing cannot take place in case of a solid source, since the low energy electrons are stopped in the source material. Another consequence of the higher intensity of the injected beam is the increasing size of the ion cloud due to space charge effects [15] and correspondingly a reduction in trapping and detection efficiency. The larger size of the ion cloud also results in a larger number of electrons striking closer to the detector edge and a higher probability for the electron escape. One can calculate from the intensities of the electron lines, the estimated yields for both isomeric beams and from the known electron conversion coefficients that the trapping and detection efficiency for ^{118}In is a factor of 5 smaller than for the corresponding ^{116}In beam.

An additional factor influencing the resolution and background can be an accumulation of electrons emitted at large angles with respect to the trap axis and trapped

between the magnetic mirrors on both sides of the trap. Furthermore the trapping of the decay products, that have a high charge [16] and low recoil energy with respect to the trapping potential (200-300 V) can influence the spectra of the conversion electrons.

It is interesting to compare the spectrum in Fig 5b with an in-trap spectrum collected for the thinnest available implanted ^{131}Ba solid source (Fig. 3c). As it is seen from the figures even with worse energy resolution and with the strong background from the accelerated stray electrons, the spectrum from the trapped ions exhibits a better peak to background ratio and a line shape without typical low-energy tail and low-energy plateau from scattered electrons.

Unfortunately, it was not possible during this short test, that was performed in parasitic mode with respect to another experiment using the ISOLDE separator, to perform more systematic studies of the obtained spectra. However, the feasibility of in-trap spectroscopy was demonstrated.¹⁾

2.4 Off-line experiments.

2.4.1 The spectroscopy of α -decaying ^{221}Fr

With the intense schedule of the REX-ISOLDE commissioning [18] we did not have the opportunity to perform further on-line tests during the 2001 year. However, an off-line experiment was performed after the annual shutdown of the CERN accelerators. An UC target with a surface ion source was installed at the mass separator. The target-source assembly has been used in previous experiments, therefore it still contained a large amount of ^{225}Ac ($T_{1/2}=10.0$ d) and other long-lived isotopes, produced by spallation reactions during the bombardment of the target with the proton beam. The target was heated to 2000 °C and ^{221}Fr atoms ($T_{1/2}=4.9$ min), produced in the α -decay of ^{225}Ac , diffused through the target's bulk and got ionised in a heated tungsten ioniser tube. The yield of the mass-separated ^{221}Fr was found to be $5 \cdot 10^6$ atoms per second. This value should be corrected by 80% beam transport efficiency and 40% efficiency of the beam injection into the trap. Like in the Indium measurements the parameters of the trap were first optimised with the MCP diagnostics. A ^{223}Ra beam ($T_{1/2}=11.3$ d) which has an intensity of one order of magnitude higher than the ^{221}Fr beam was used. After the optimisation the detector assembly was introduced into the trap and ^{221}Fr was injected. The beam was accumulated and cooled simultaneously. A typical electron spectrum taken for 5 seconds of accumulation is shown in Fig 6 (spectrum 1). One can observe the 60 keV line corresponding to accelerated stray electrons as well as K-, L- and unresolved M,N- electron transitions from the 218 keV level in ^{217}At populated in the α decay of ^{221}Fr . A weak 83 keV L-line from the 100 keV transition is also visible. As it is seen from Fig. 6 the resolution for the 122 keV K-line is about 2 keV. This is better than the in-trap measurements with solid sources (Fig 3c). The resolution for L- and M,N-lines is worse due to the multiplet character of these transitions. The intensity ratio of K-, L- and unresolved M,N lines is 1: 1.17(3):0.39(3). This can be compared with theoretical ratios 1:1.23:0.43 [19] obtained with the assumption of E2 multipolarity for the 218 keV γ -transition.

A new feature in the spectrum is the strong low-energy background that was not observed in the case of trapped isomers (Fig. 5ab). This background is also not observed in a measurement with a solid ^{221}Fr source [20]. The recoil energy of the ^{217}At α -decay products is of the order of 100 keV. One consequence of nuclear decay can be a sudden

¹⁾ Results of this test were also reported briefly in [17].

creation of a vacancy in the inner electronic shell followed by a cascade of several atomic electrons. An average ion charge of decay products with $Z \approx 85$ is around 9-13 depending on the shell where the vacancy was produced [21]. The high charge of such recoils corresponds to a relatively small radius (≈ 2 mm) of the spiral trajectory in the magnetic field of the trap. Additionally the kinetic energy of the recoils, unlike the case of β and IT decays, is high enough to overcome the shallow electrical trapping potential. Therefore a significant fraction of the recoils is transported to the detector, penetrates the 2500 nm dead layer and leaves a signal in the low-energy part of the energy spectrum. The energy distribution of the 100 keV decay products that passed the detector dead layer at various incident angles can be estimated using the SRIM code [22]. The calculations show that the majority of the recoils deposit energy in the 20-30 keV range depending on the incident angle. From the ratios of the intensities of the conversion electron lines and the low-energy background one can estimate the probability for the creation of a vacancy as 15 %. This value is of the same order of magnitude as the typical probability of electron shake-off as a consequence of β -decay [23].

It is interesting to compare this spectrum to a spectrum corresponding to a longer collection time of 30 minutes (Fig 6, spectrum 2). One can observe that while the shape of the 60 keV stray electron line does not change, the resolution for the conversion electron lines degrades significantly. The conversion electron lines exhibit a low-energy shift and a strong low-energy tail. This agrees with the observations from the previous chapter that the saturation of the trap causes a deterioration of the quality of electron spectra.

The spectrum taken for longer collection time also exhibits the conversion electrons and β continuum from ^{213}Bi ($T_{1/2}=44.9$ min.), the grand-daughter of ^{221}Fr (this background was subtracted from the spectrum in Fig 6). The background persists after stopping of the beam. It is reasonable to assume that the ^{213}Bi activity originates from ^{217}At daughter recoils implanted into the detector. The comparison of integrals of the ^{213}Bi conversion electron lines in the background spectrum without the beam with the low-energy recoils contribution in the collection spectra also supports this assumption.

2.4.2 The detection of conversion electrons as a tool for trap diagnostics.

The detection of conversion electrons can be useful for studying the trap performance.

From the intensities of the electron lines of ^{221}Fr , the known conversion coefficients and in-trap detection efficiency, and from the measured yield a trapping efficiency of the order of 2.5% can be obtained. This trapping efficiency is much smaller than the ones quoted in [15] ($\approx 20\%$). Those measurements were done for short accumulation times and a small amount of accumulated ions (10^4). The authors also observed that the trapping efficiency drops significantly with the number of accumulated ions due to space-charge effects. Therefore the low efficiency in our test is most likely due to the high yield of injected ions and the long accumulation times.

We have performed several series of short measurements where the counting rate of the conversion electrons was measured as a function of various trap parameters. After each short measurement the trap was cleaned by applying the magnetron frequency. No ^{221}Fr signal was observed after this.

To obtain information on the ion survival time inside the trap a few measurements were done for the same collection time of 10 seconds and various measurement times. The recording of the electron spectrum and collection of ions in the trap were started simultaneously. As a result one can say that the ^{221}Fr signal stops very promptly after

the ion collection. This indicates that the ions survive in the trap only for a short time of the order of a second ²⁾.

The dependence of the conversion electron rate on the value of the radio frequency for centering the ions is shown in Fig 7. One can observe from the figure that the resonance is quite broad. Its centre is shifted approximately by 3 kHz from the value calculated from the magnetic field strength. A similar high-frequency shift was reported in measurements with stable ions [15]. Using the dependence of the resonance shift on the number of trapped ions [15] one can estimate that the number of trapped Fr ions was about $2.5 \cdot 10^6$. This number is consistent with a saturation value reached with the intensity of the injected ions and the estimated ion survival time in the trap. The same value can be deduced from the efficiency value mentioned above.

Changing the voltage on electrodes in the trap centre the position of the ion cloud relative to the trap centre can be shifted. As the radius of the spiral of the electron trajectories in the trap is only a fraction of a millimetre, an information on the cloud size can be obtained by monitoring the electron counting rate as a function of the ion cloud position. The dependence of the counting rate on vertical and horizontal shifts are presented in Fig 8ab. From this measurement the effective diameter of the ion cloud can be estimated as ≈ 3.5 mm.

In principle, the introduction of a segmented detector or an MCP with a camera into the trap may allow to obtain a detailed image of the ion cloud using the conversion and atomic electrons, the same way as secondary electrons can be used for imaging of solid radioactive sources [24].

The normalised rates of conversion electrons and low-energy background as a function of buffer gas pressure in the centre of the trap are presented in Fig. 9. One can observe that while the rate of conversion electrons stays practically constant within the investigated pressure range, the number of low-energy counts changes dramatically. Such a behaviour confirms the suggested origin of the low-energy background as the highly-charged α -decay recoils, which are transported to the detector. The scattering and charge-exchange reactions with buffer gas atoms are many orders of magnitude higher for the heavy highly-charged ions [25] compared to energetic electrons [26]. The consequent reduction of the ion charge results in an increase of the ion's spiral radius and, hence, a reduction of the transport efficiency to the detector. More systematic studies are required to achieve a better understanding of the complicated interactions between decay products and buffer gas atoms.

The reduction of the energy resolution and counting rate in conversion electron lines was also observed for high buffer gas pressure.

3 Conclusion

We have demonstrated the feasibility of in-trap electron spectroscopy using the Penning trap REXTRAP. Although REXTRAP is not an ideal choice for such an experiment, spectra with good resolution of conversion electron lines and peak to background ratio were obtained. The quality of the spectrum deteriorates dramatically with overloading the trap. To achieve good resolution it is important to keep the number of trapped ions lower than a certain limit ($\approx 10^6$ atoms), that also corresponds to a smaller size of the ion cloud and a higher value of the trapping efficiency. The stray electrons, accelerated

²⁾ The short time that ions spend in the trap does not create a problem for REX-ISOLDE, since the facility was designed for much shorter accumulation times (≈ 20 ms) [7].

by the trap's high-tension, cause background in the energy spectrum. The trapping of electrons and low-energy decay products due to the magnetic mirror effect of the maxima in the magnetic field distribution at the two ends of the trap may influence the quality of spectra. A high buffer gas pressure results in a deterioration of the electron line resolution. In the case of trapping α -emitting nuclei the recoiling decay products cause a significant low-energy background. The daughter activity of recoils implanted into the detector also present a background problem.

Together with a small detector the detection of conversion electrons can be used as a simple trap diagnostics tool and proved to be useful for better understanding and, eventually, improvement of the trap performance. The obtained results are consistent with earlier measurements performed with stable beams.

Further systematic investigations of the rich possibilities opening up with in-trap electron spectroscopy will follow.

We wish to acknowledge Dr. M. Dietrich for technical assistance and help in the preparation of the ^{131}Ba source. We are grateful to Dr. U. Köster, Mr. R. Catherall and the ISOLDE technical group for help in the operation of the ion source and the mass-separator. This work was supported by the EXOTRAPs project.

References

- [1] H.H. Jorch, J.L. Campbell, Nucl. Instr. and Meth. **143** (1977) 551.
- [2] J.L. Campbell and H.H. Jorch, Nucl. Instr. and Meth. **159** (1979) 163-170.
- [3] G.T. Ewan and L. Graham, in "Alpha- Beta- Gamma-ray Spectroscopy", edited by K. Siegbahn, North-Holland publishing company (1965).
- [4] J.M. Hollander and D.A. Shirley, Ann. Rev. Nucl. Science, 1970
- [5] M. S.Freedman, Ann. Rev. Nucl. Science, 1974
- [6] F. Ames, G. Bollen, G. Huber, P. Schmidt, Proceedings of ENAM98.
- [7] D. Habs *et. al*, Nucl. Phys. **A616** (1997) 29-38.
- [8] G. Bollen *et. al*, J. Appl. Phys. **68** (1990) 4355-4374.
- [9] E. Kugler, Hyp. Int. **129** (2000) 23.
- [10] SIMION 3D Vers. 7.0 Idaho Nat. Engineering and Enviromental Lab. (2000).
- [11] J. Kalef-Ezra, Y.S. Horowitz and J.M. Mack, Nucl. Insr. and Meth. **195** (1982) 587-595.
- [12] W.H. Trzaska, Nucl. Instr. and Meth. **A297** (1991) 504-511.
- [13] D.J. Horen, J.M. Hollander and R.L. Graham, Phys. Rev. **135** (1964) 301.
- [14] J.M. Parmonen *et. al*, Nucl. Instr. and Meth. **A306** (1991) 504-511.
- [15] F. Ames, P. Schmidt, O. Forstner, G. Bollen, O. Engels, D. Habs, G. Huber, Hyp. Int. **132** (2001) 469.
- [16] A.H. Snell and F. Pleasonton, Phys. Rev. **107** (1957) 740.
- [17] L. Weissman, F. Ames, J. Äysto, , O. Forstner, S. Rinta-Antila and P. Schmidt, Hyp. Int. **132** (2001) 535.
- [18] O. Kester *et. al*, proceeding of PAC2001, Chicago Illinois, June 18-22, 2001.
- [19] F. Rösel, H.M. Fries, K. Alder, H.C. Pauli, At. Data Nucl. Data Tables 21 (1978) 91.
- [20] R.K. Sheline, C.F. Liang and P.Paris, Phys. Rev. C **51** (1995) 1192.
- [21] T.A. Carlson, W.E. Hunt and M.O. Krause, Phys. Rev. **151** (1966) 42.
- [22] J.F. Ziegler, J.P. Biersack, U. Littmark, The Stopping Power and Ranges of Ions in Solids, Pergamon press, New-York, 1985.

- [23] T.A. Carlson, C.W. Nestor, T.C. Tucker and F.B. Malik, Phys. Rev. **169** (1968) 169.
- [24] L.Weissman, K. Krougov, M. Huyse, P. Van den Bergh, P. Van Duppen, Nucl. Instr. and Meth. **A452** (2000) 147.
- [25] A. Müller and E. Salzborn, Phys. Let. **A62** (1977) 391.
- [26] Y.S. Kim and R.H. Pratt, Phys. Rev. **C27** (1983) 2913.

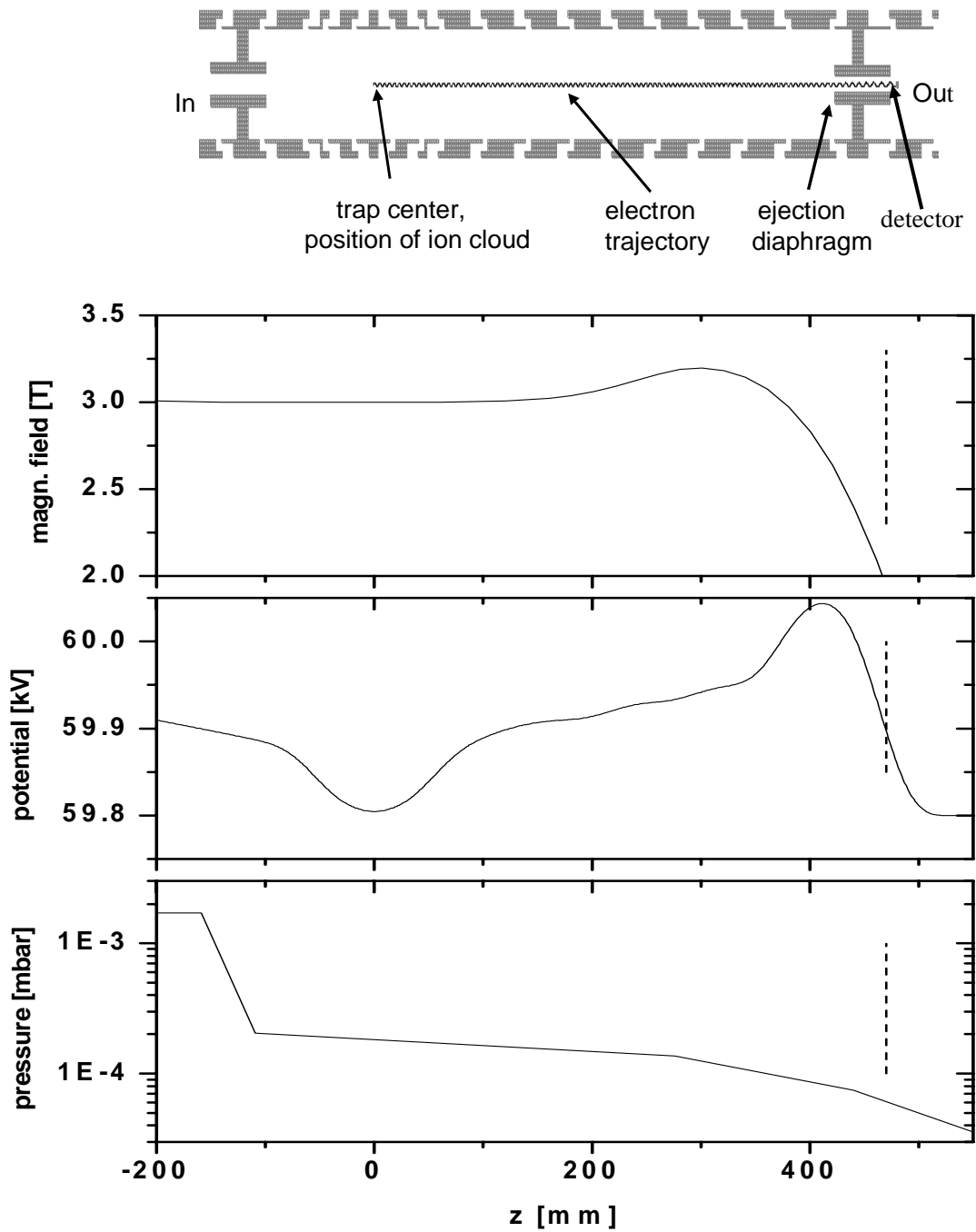


Figure 1: General overview of the inner part of REXTRAP together with an example of a simulated trajectory of a 400 keV electron. The typical distribution of buffer gas pressure and the trapping electric potential is also shown together with the magnetic field profile.

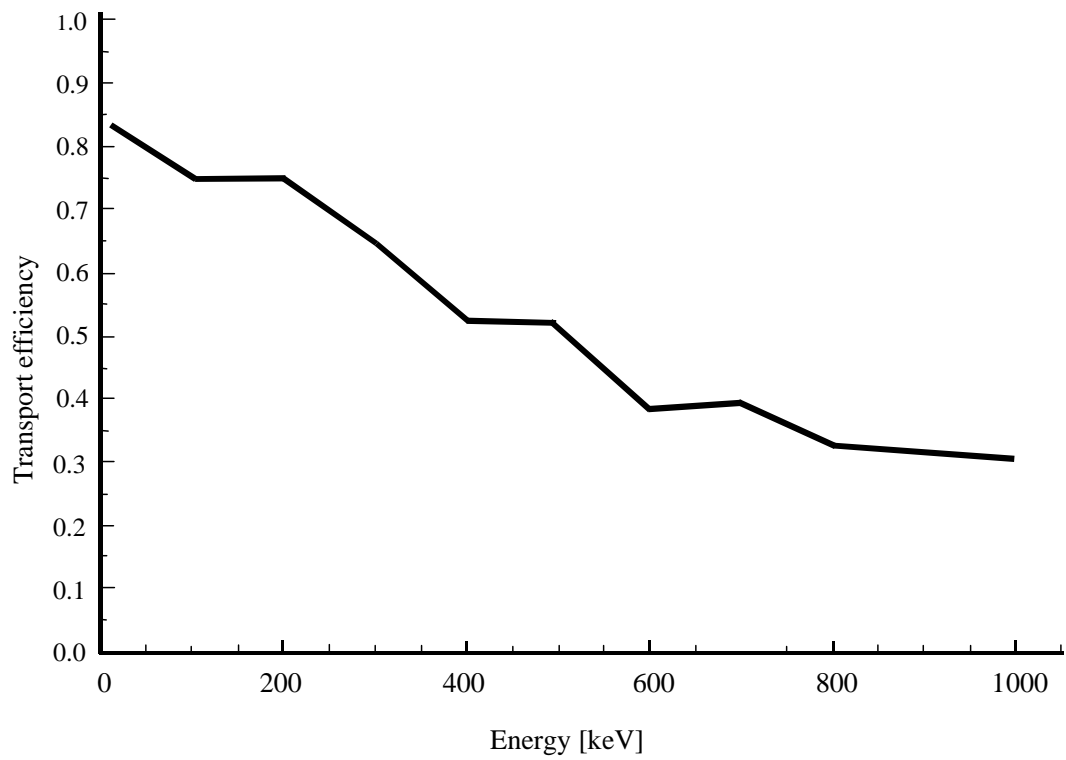


Figure 2: Calculated probability for electrons emitted in the forward direction from the centre to hit the detector. The diameter of the source was taken to be 1 mm.

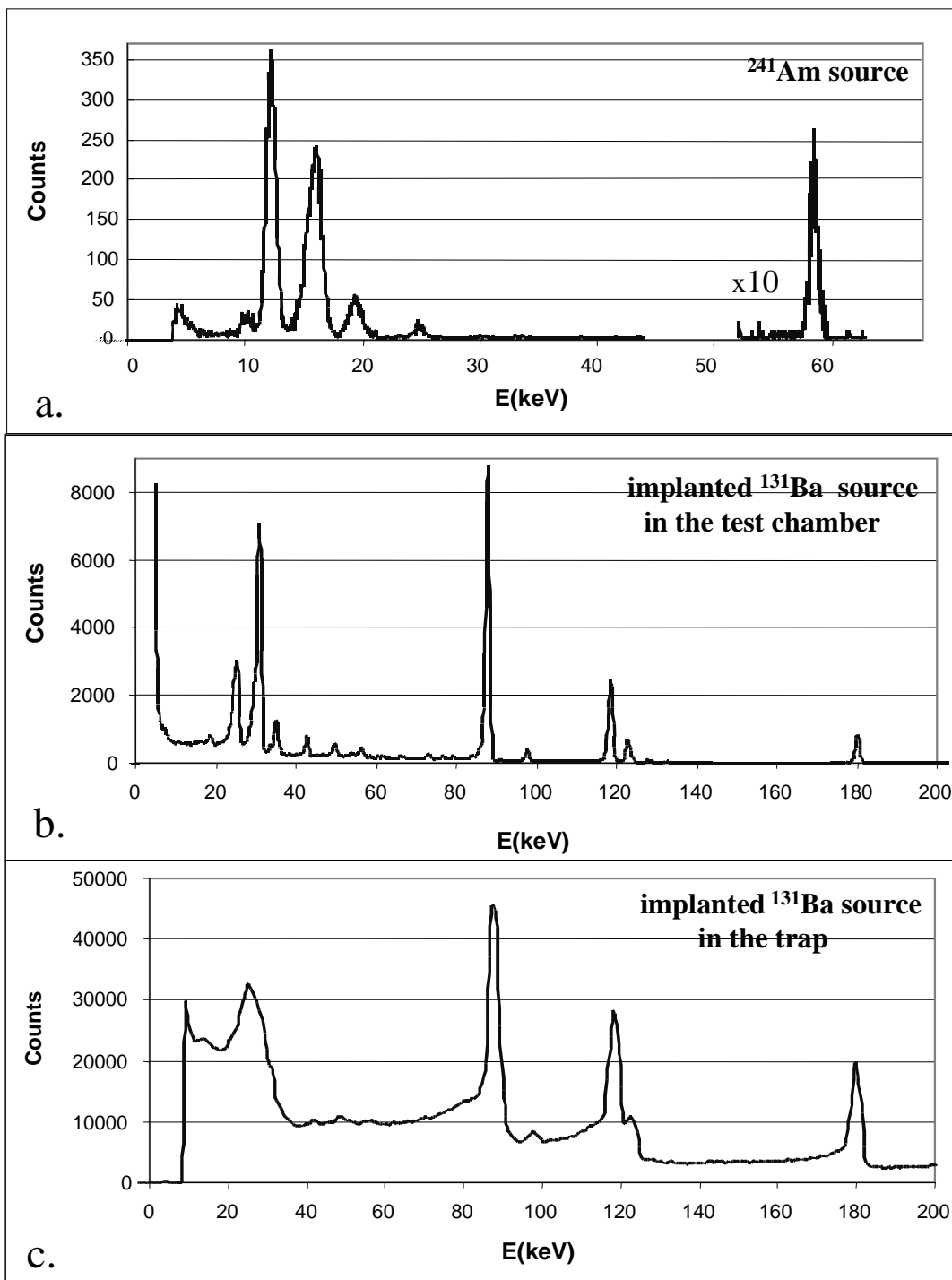


Figure 3: a. X-ray spectrum of a ^{241}Am source, b. spectrum of a ^{131}Ba source produced by implantation of the 60 keV ISOLDE beam into a thin aluminium tape. The spectrum was taken in a test chamber without magnetic field. c. spectrum of the same ^{131}Ba source taken in the magnetic field of the trap.

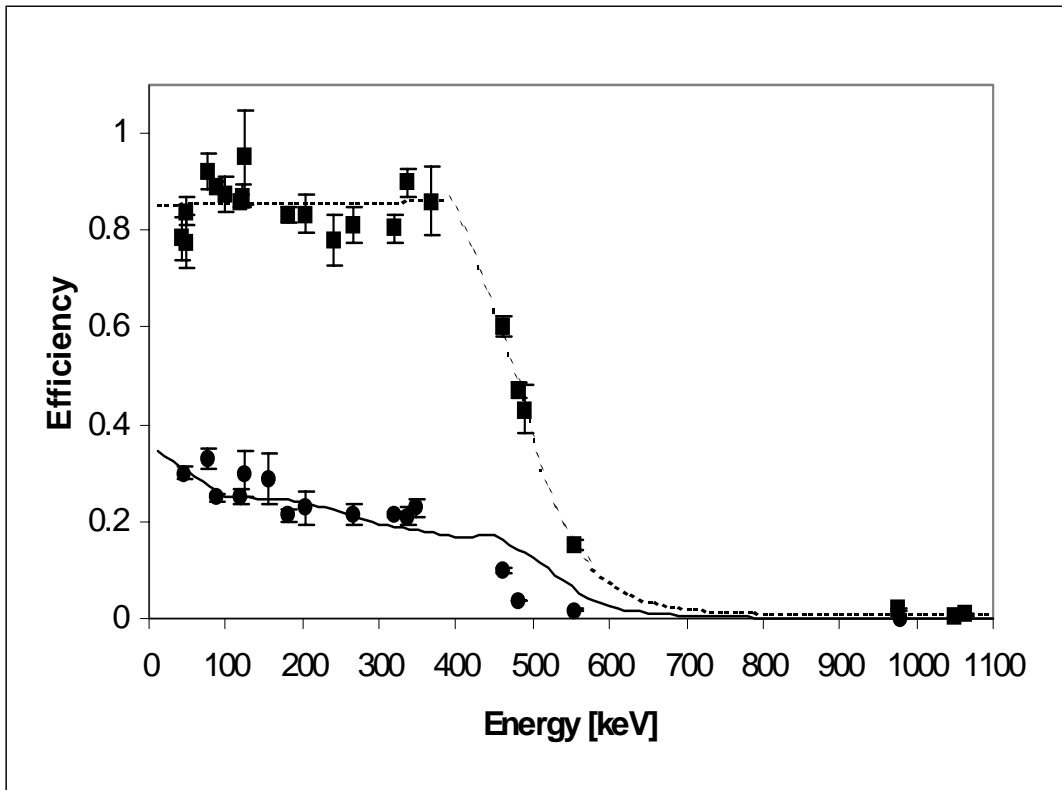


Figure 4: Experimental (circles) and calculated (solid line) detection efficiencies for measurements in the magnetic field of the trap. The squares and the dashed line represent the experimental intrinsic detector efficiency measured in the test chamber without magnetic field.

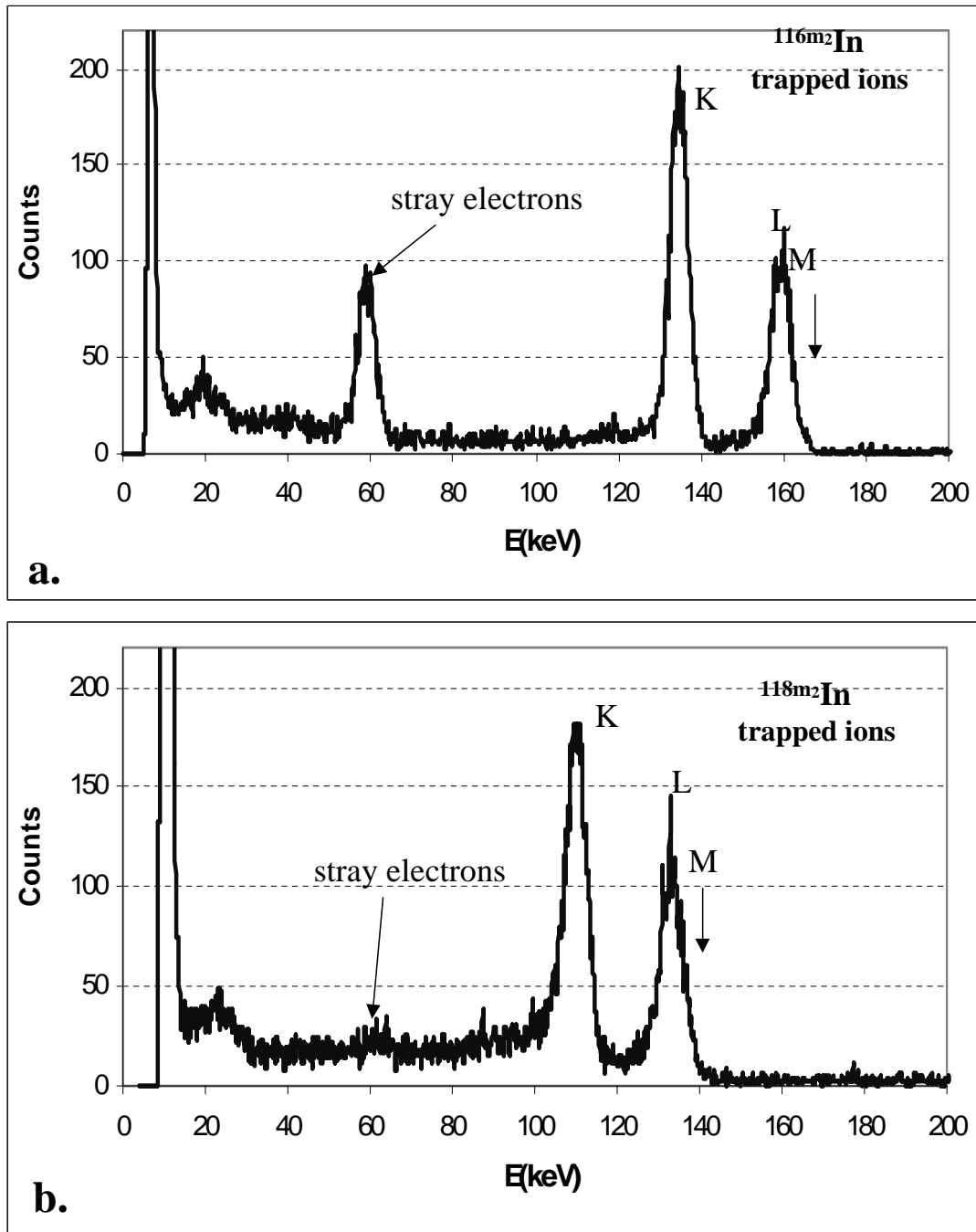


Figure 5: a. spectrum collected from $^{116m2}\text{In}$ trapped isomers, b. spectrum collected for $^{118m2}\text{In}$ trapped isomers for the same trapping cycle.

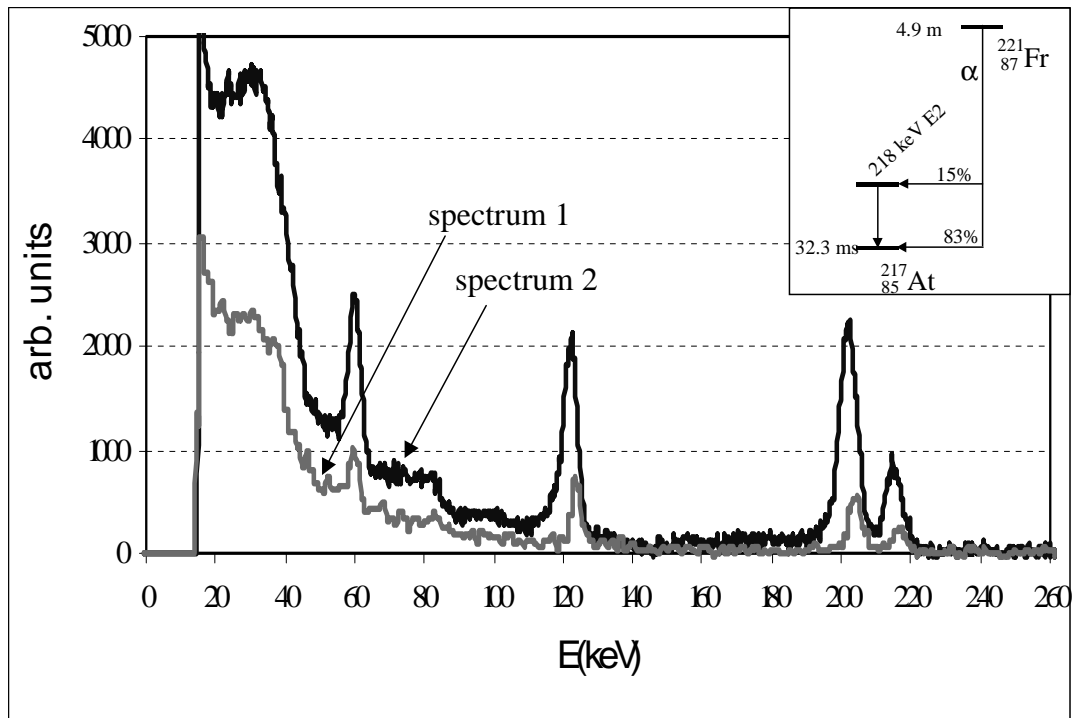


Figure 6: Two arbitrary normalised spectra from the trapped ^{221}Fr ions taken for a 5 second collection (spectrum 1) and for a 30 minutes collection (spectrum 2). The first spectrum is binned with a factor 3.

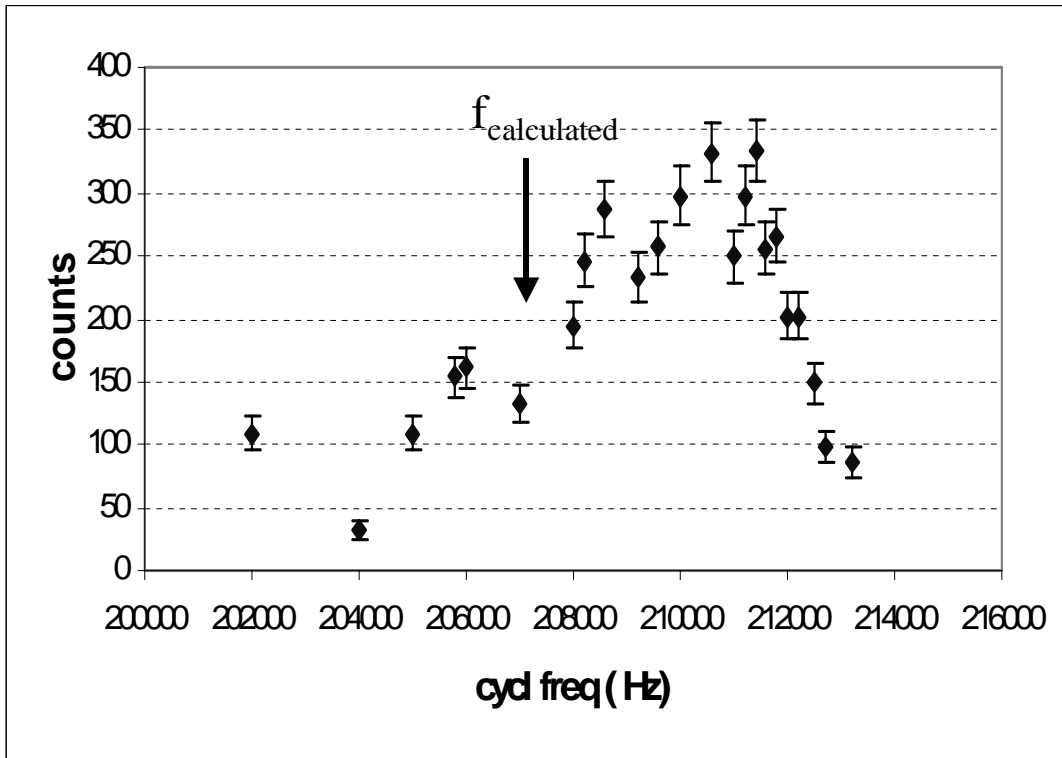


Figure 7: Dependence of the conversion electron rate as a function of the applied radio-frequency for centering the ions. The calculated cyclotron frequency is indicated.

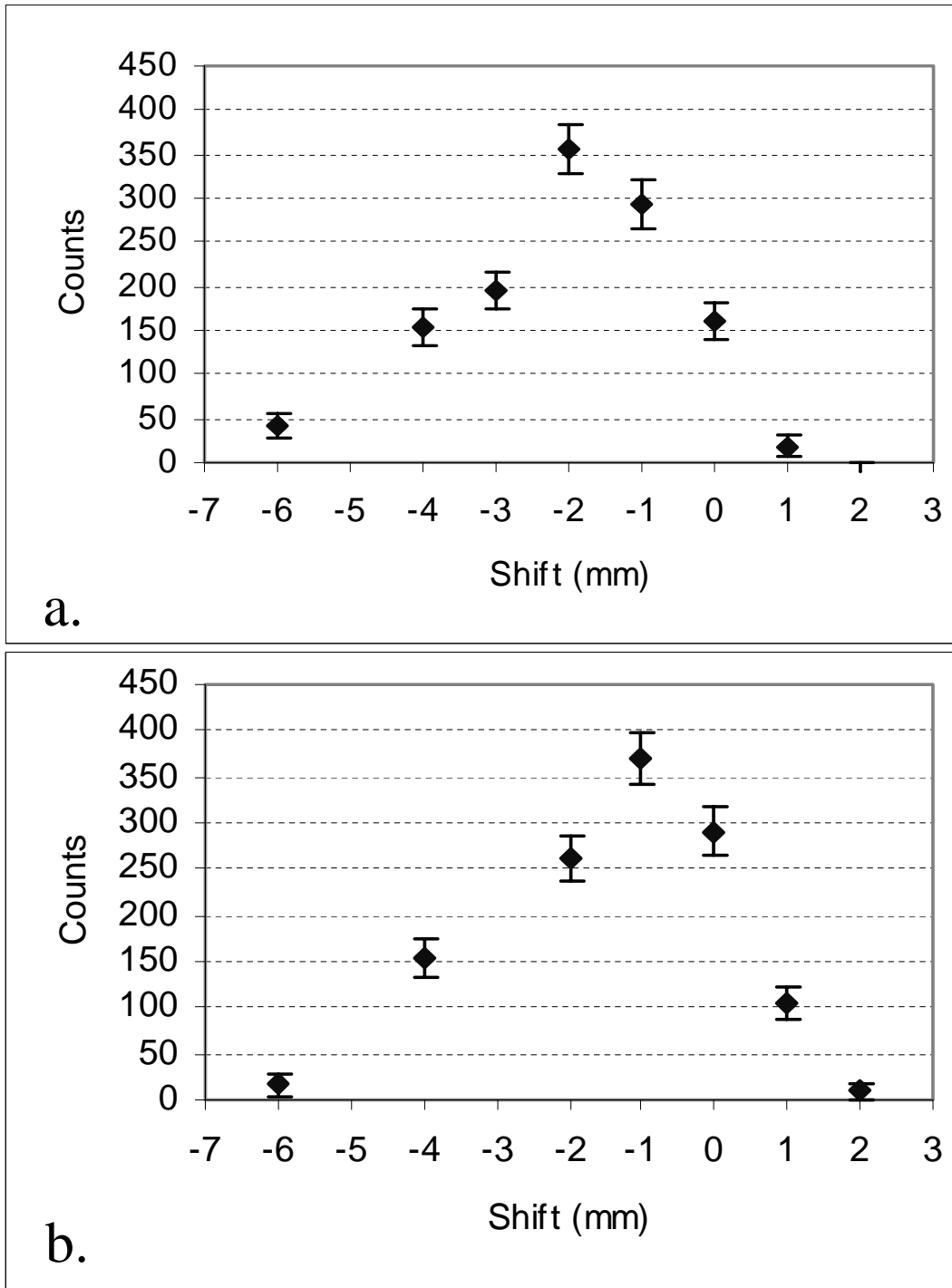


Figure 8: Dependence of the conversion electron rate as a function of the cloud position relative to the trap centre in vertical and horizontal direction.

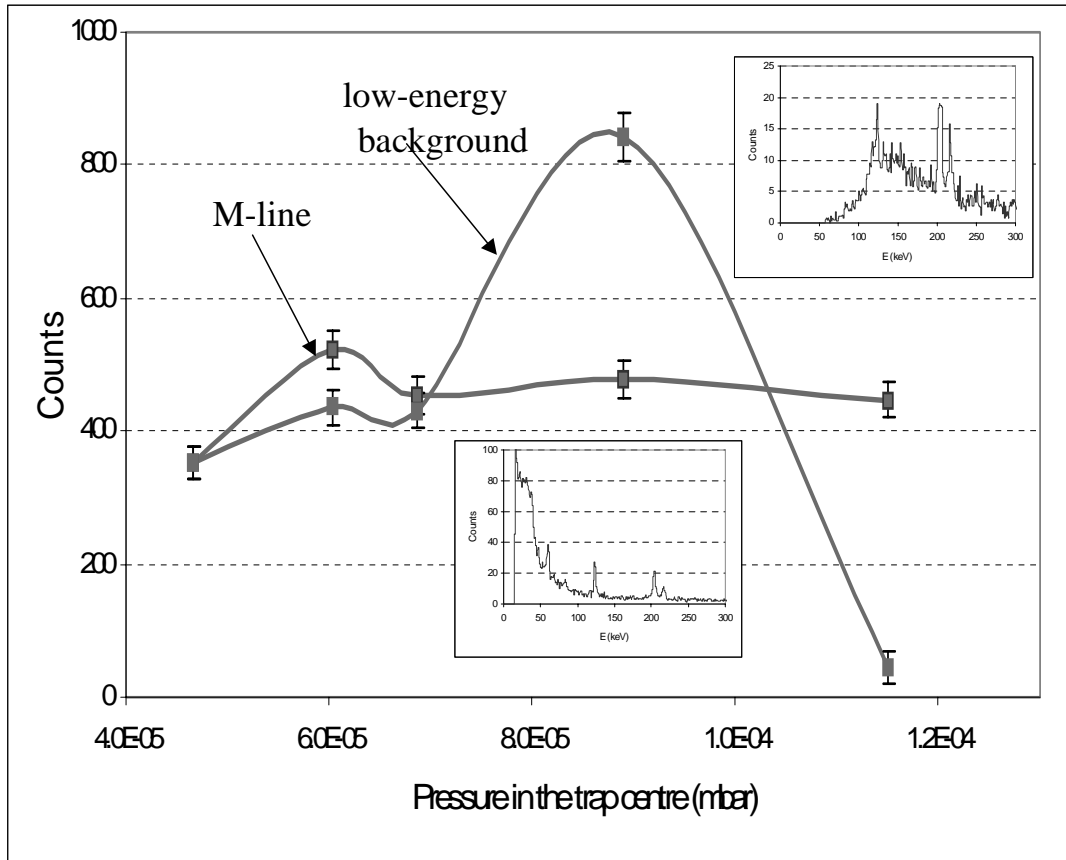


Figure 9: Dependence of conversion electron and low-energy background rates as a function of the buffer gas pressure in the trap centre. Spectra corresponding to the buffer gas pressure of $9 \cdot 10^{-5}$ and $1.15 \cdot 10^{-4}$ mbar are shown in the inserts.